NACA RM E51L17

NACA

RESEARCH MEMORANDUM

A PHOTOGRAPHIC STUDY OF FREEZING OF WATER DROPLETS FALLING FREELY IN AIR

By Robert G. Dorsch and Joseph Levine

Lewis Flight Propulsion Laboratory
Cleveland, Ohio

NATIONAL ADVISORY COMMITTEE
FOR AERONAUTICS

WASHINGTON

February 25, 1952

NATIONAL ADVISORY COMMITTEE FOR AERONAUTICS

RESEARCH MEMORANDUM

A PHOTOGRAPHIC STUDY OF FREEZING OF WATER DROPLETS FALLING FREELY IN AIR

By Robert G. Dorsch and Joseph Levine

SUMMARY

A photographic technique for investigating water droplets of diameter less than 200 microns falling freely in air at temperatures between 0° and -50° C has been devised and used to determine:

(1) The shape of frozen droplets

(2) The occurrence of collisions of partly frozen or of frozen and liquid droplets

(3) The statistics on the freezing temperatures of individual free-falling droplets

A considerable number of droplets were found to have a nonspherical shape after freezing because of various protuberances and frost growth, and droplet aggregates formed by collision. The observed frequency of collision of partly frozen droplets showed good order of magnitude agreement with the frequency computed from theoretical collection efficiencies. The freezing temperature statistics indicated a general similarity of the data to those obtained for droplets frozen on a metallic surface in previous experiments.

INTRODUCTION

The presence of supercooled droplets in clouds is the primary factor responsible for the aircraft icing hazard; consequently, a complete knowledge of the physical conditions under which supercooled clouds may exist, and the factors that cause a supercooled cloud to transform to an ice-crystal cloud is necessary. A knowledge of the factors causing the transformation of a supercooled cloud to an ice-crystal cloud is of importance because ice-crystal clouds, in general, do not present an aircraft icing hazard. In addition, the occurrence of precipitation from a cloud in the form of rain or snow is usually preceded by the crystallization of a portion of the cloud.

The complexity of the problem has necessitated, to date, primarily a laboratory approach from which useful physical data have been obtained in the past several years. The behavior of supercooled water in bulk and in the form of droplets supported on thermocouples or metallic surfaces has been extensively investigated (references 1 to 4). In addition, laboratory investigations of supercooled droplets supported by air have been made, but these have been largely confined to determining the conditions under which liquid-droplet clouds transform to ice-crystal clouds (references 5 to 7). Studies of the transformation of individual free-falling liquid droplets to ice have not been made in any great detail for droplets in the size range (less than 200 μ in diam.) found in icing clouds.

Water droplets falling freely in air at temperatures between 0° and -50° C were investigated photographically at the NACA Lewis laboratory to determine:

(1) The shape of frozen droplets

(2) The occurrence of collisions of partly frozen or of frozen and liquid droplets

(3) The statistics on the freezing temperatures of individual free-falling droplets

APPARATUS

A schematic drawing of the apparatus for observing the presence of frozen droplets among free-falling droplets is shown in figure 1. The entire apparatus, with the exception of the temperature recording device, was housed in a large cold chamber (inside dimensions approximately 10 ft long, 7 ft wide, and 10 ft high). A photograph of the apparatus in place in the large cold chamber is shown in figure 2. The apparatus consisted of a heated spray chamber from which droplets settled into a cooled 4- by 4-inch vertical duct. The cooled droplets were photographed with a camera and spark source as they passed windows at the bottom of the duct after a $4\frac{1}{2}$-foot fall. Provision was made for pumping air out through one end of the spray chamber, so that an upward flow of cold air from the cold chamber could be imposed in the vertical duct.

The spray chamber was kept at temperatures above freezing by a copper steam pipe soldered to the walls of the chamber. Similarly, in order to prevent the water pipes from freezing, the steam pipes were conducted to and from the spray chamber in contact with the water lines. The heated portions of the apparatus were insulated with felt to minimize heat losses. Both the spray chamber and vertical duct were made from Inconel metal to avoid corrosion.

Thermocouples were installed in the spray nozzles for measuring the water temperature. The air temperature in the cold vertical duct was measured at three vertical positions (top, center, and camera level) by pumping air from the duct past thermocouples housed in 3/4-inch diameter tubes attached to a wall of the duct. Glass-wool filters prevented stray droplets from striking the thermocouples. The mass-flow rate of the air pumped from the duct was obtained from the area of the thermocouple-housing tube and the local static pressure in the housing tube measured by a micromanometer. Low mass-flow rates were used in order not to disturb appreciably the air in the duct. The temperatures were recorded on a strip-chart self-balancing potentiometer placed outside the large cold chamber.

The lens of the camera used to photograph the cooled droplets was similar to those used in motion-picture cameras and had a focal ratio of f/2.8 and a focal length of 2 inches. The depth of field was approximately 0.4 millimeter and the volume of field was 0.036 cubic centimeter. The image distance was approximately 44 inches and the magnification was 22X. The depth of field and the magnification were measured by taking photographs of a group of fine quartz fibers placed successively at greater distances from the face of the camera lens. The accuracy of the diameter measurements varies from ± 5 percent at 100 microns to ± 10 percent at 10 microns. Bright field illumination was furnished by a spark source located on the opposite side of the vertical duct from the camera. The spark source and its power supply are described in references 8 and 9. The spark duration was approximately 2 microseconds, which was a sufficiently short exposure time to yield sharp droplet images.

Droplet photographs were taken with fast orthochromatic 8- by 10-inch film. Long development time (10 min) was found to be necessary in order to give sufficient contrast. The images of the droplets appeared on the negatives as white areas on a dark background. Many of the droplet images had dark spots in the center, which were images of the spark source formed by the droplets. A positive photograph of the droplets at room temperature taken with this apparatus is shown in figure 3.

An upward flow of cold air from the chamber could be imposed in the vertical duct in order to slow the rate of fall of the droplets and thereby to obtain a longer cooling time before the droplets were photographed. The air outlet from the spray chamber narrowed from a 4- by 4-inch cross-sectional area in the duct to 1- by 1-inch. Thus the airflow velocity was increased in the constricted portion of the outlet to a value which could be measured by total and static tubes connected to a micromanometer.

The foregoing arrangement permitted the required control and rough measurement of low vertical-air velocities. Inasmuch as the pressure differential for the velocities used was only of the order of 0.02 inch

of water in the 1- by 1-inch section, a precise measurement of velocities was difficult by this method. A more accurate determination of the duct velocity was obtained from the terminal velocity calculated for the smallest droplet appearing in the duct as determined from the droplet photographs.

PROCEDURE

Droplet temperature. - A direct measurement of droplet temperature was not possible with the apparatus just described, but a computation of how close a droplet of a given size will approach the cold air temperature of the duct in dropping from the warm spray chamber to the camera window level in the vertical duct (127 cm) was possible. The method used for making these computations is described in appendix A. The computed results are summarized in figure 4, which indicates that droplets 200 microns or less in diameter have a temperature negligibly different from air temperature at camera level in the duct. The duct air temperatures measured by the thermocouples at the midpoint and at camera level were usually the same (within 1° C). The temperature measured by the upper thermocouple was somewhat higher (2° to 3° C) because of the proximity of the heated spray chamber.

Detection of frozen droplets. - In addition to determining the temperature of the droplets it was desirable to find a means of differentiating a frozen droplet from a supercooled liquid droplet. A previous investigation showed that a droplet suspended from a thermocouple and observed in bright field illumination generally forms a crude image of the light source, which appears in the positive photographs as a bright spot at the center of the dark circular droplet image. The freezing of a supercooled droplet thus suspended was detected by the disappearance or marked decrease in intensity of the bright spot at the center of the droplet image in an investigation in 1948 by John C. Johnson at Massachusetts Institute of Technology. Investigations at the NACA Lewis laboratory substantiate this method for use with droplets suspended from a thermocouple. Because similar bright spots occur in the images of free falling droplets photographed with the camera, an attempt was made to use the foregoing criterion for determining when free falling droplets were frozen.

An examination of the droplet images on the photographic negatives disclosed that a considerable portion of the images had a noncircular outline. For reasons, discussed in the Results and Discussion section, these noncircular images were considered to be indicative of frozen droplets. However, considerable numbers of these noncircular images had bright spots at the center. This obvious contradiction coupled with the apparent reliability of the noncircular image criterion eliminated

frozen-droplet detection by the bright spot method. Although noncircular droplet images are definite indicators of frozen droplets, an unknown portion of circular droplets may also be frozen. Circular images may be produced by nonspherical (and thus frozen) droplets because of their particular orientation to the camera. Inasmuch as neither the portion of the circular droplet images that are due to unfrozen spherical droplets nor the portion due to droplets that are frozen and remained spherical is known, any absolute estimate of the ratio of frozen to unfrozen droplets in a particular sample is impossible. An appraisal of the ratio of noncircular droplets to the sum of the circular plus noncircular droplets was therefore made as the best means available to detect droplet freezing trends.

Range of conditions. - Droplet photographs were taken at various temperatures ranging from 0° to -51° C. A group of droplet photographs were also taken at room temperature (approximately 20° C) for comparison with those taken at temperatures below 0° C. For droplets between 46 and 200 microns in diameter, the temperature range below 0° C was completely covered by photographs taken with an updraft velocity in the duct of approximately 7 centimeters per second (terminal velocity for a 46-micron droplet). Because of current interest in the rate of formation of ice crystals in the temperature region of -40° C, the temperature range from -36° to -48.5° C was also covered by droplet photographs taken with no updraft in the duct. For this range, inasmuch as no updraft was used, it was possible to extend the lower limit of the droplet diameter range from 46 to 5 microns.

RESULTS AND DISCUSSION

Shape of frozen droplets. - Observations at room temperature indicated unfrozen droplet images were always circular in outline (fig. 3). In photographs of droplets below -20° C, a considerable number of noncircular droplet images was noted (fig. 5). In general, two broad types of noncircular droplet image were observed: type I, images of aggregates of droplets that apparently froze together (for example, droplets 5, 6, and 7 of fig. 6 and 5 of fig. 7); type II, images of irregularly shaped droplets with various types of protuberance (for example, droplets 1, 2, 3, 17, 18, 21, and 24 of fig. 6). Many images were found that were combinations of the two types (such as droplet 33, fig. 6).

The droplet images have been classified with respect to size and type of image and the results are tabulated in tables I and II. The images that were considered as combinations of the two types were included in the type I group. The sorting of droplet images into type I and type II categories was complicated by the poor definition of the smaller protuberances in the photographs making the boundary line

between the two types rather indistinct. The noncircular droplet images were therefore examined with a low powered microscope and only those irregularities which had a definitely circular outline were considered as caused by collision. The remaining protuberances were included in the type II group.

Computations of probabilities of collisions between droplets of different sizes and hence different terminal velocities have been made (appendix B). These computations yielded results consistent with the hypothesis that type I images are the result of collisions between partly frozen droplets. The type II images were probably caused by droplets that were distorted because of internal forces created during freezing and by frost growth on the frozen surface of the droplets.

Noncircular images of both types occurred more frequently in the absence of vertical air velocity in the duct than with vertical air velocity. This difference is shown in a comparison of tables I and II. The vertical air velocity in the duct prevented the smaller droplets from entering the vertical duct, therefore the frequency of collision was reduced (appendix B). Thus, noncircular type I images are obviously greater in number with no vertical air velocity present; however, the presence of a greater number of type II images under the same conditions is not as readily explained. A reasonable explanation may be obtained by considering the factors that may cause protuberances to form. Pointed protuberances, or spicules, have been observed on the frozen surface of small samples of water cooled in glass bulbs (reference 1), on droplets that were frozen while suspended from a thermocouple in the investigation by Johnson, and on the surface of sleet pellets (reference 10). It is suggested in reference 1 that the spicules were formed because of internal pressure created by the freezing of the surface layer first and subsequent rupture of the surface ice at a weak spot followed by supercooled water issuing through the break and forming a tube that freezes. Similarly, when a small supercooled droplet freezes, particularly if the freezing starts as a shell over the surface, pressures and strains undoubtedly arise within the body of the droplet and may cause pointed protuberances or other irregularities to form at weak spots on the frozen droplet surface. The fact that images of the light source (bright spots) were found associated with many images of frozen droplets in the data of this report indicates that freezing may have been taking place primarily in the surface shell leaving liquid in the center for a period of time. Droplets frozen on thermocouples or on metallic surfaces usually have a milky appearance due to the network of many dendritic crystals formed within. This type of ice would cause considerable scattering of transmitted light and the refracted light would probably be of insufficient intensity to cause a bright spot at the center of the droplet image. If, however, only a thin ice shell formed first, leaving considerable clear liquid in the interior, a droplet would still transmit considerable refracted light at this stage. An alternative explanation is that the droplets freeze with a clear, or glassy, ice structure throughout.

In addition, in the course of work at the Lewis laboratory with droplets supported on a metallic surface much colder than the environment, supercooled droplets observed in profile have frozen from the metal supporting surface up. As the line of demarcation between ice and liquid reached the top of the droplet a pointed protuberance was observed to form there. This point acted as a root for a fragile tree-like frost structure, which grew upward into the water-saturated air above. Thus, the conception that pointed protuberances may form when free falling droplets freeze is quite plausible. Some droplets show definite evidence of the existence of such protuberances (figs. 6 and 7). Droplet images with irregular outlines due to protuberances and dendritic frost growth (type II images) were more pronounced and more numerous (compare tables I and II) when no updraft was present in the duct. This would indicate that a considerable portion of the irregularities in the shape of the droplets was due to crystalline growth due to reverse sublimation after freezing. If the surface irregularities resulted entirely from the freezing process, then duct velocity should have had no effect. The marked influence of the air velocity in the duct on the formations was apparently a reflection of the variation of vapor-pressure conditions with duct velocity.

There are two ways in which duct velocity may have affected vapor-pressure conditions within the duct. First, the air drawn up into the duct was relatively drier than the air present because it had passed over the cooling coils of the chamber, which were several degrees colder than the duct temperature. Second, inasmuch as the local vapor-pressure gradient at any point in the duct is a function of the number of droplets per unit volume and the temperature of the droplets (which is in turn a function of the size and position of the droplets in the duct), the fact that the smaller droplets were removed from the duct with the presence of an updraft also affected the vapor-pressure conditions.

On the basis of the considerations in the preceding discussion, the average vapor pressure was estimated to be roughly equal to the value corresponding to saturation with respect to ice at the duct temperature when an updraft was present. When no updraft was present in the duct, the average humidity appeared to be closer to the condition of saturation with respect to water. Thus, when no updraft was present, there was apparently an ample supply of water vapor available for the growth of dendritic frost structures on the surface of frozen droplets, particularly at protuberances.

Droplet collisions. - As previously mentioned, type I images were due to aggregates of frozen droplets which apparently cohered after colliding. Collisions between two or more droplets in the following states are possible: (1) liquid (but not supercooled) droplets in the

upper portion of the duct, (2) supercooled liquid droplets, (3) completely frozen droplets, (4) partly frozen droplets or frozen droplets with a wet surface, and (5) a frozen or partly frozen droplet with a supercooled droplet.

Inasmuch as the individual droplets in the aggregates usually roughly retained a spherical shape and the droplets cohered after collision, states (4) and (5) appear to be the most probable states before collision which would account for images of type I. It is unlikely that completely frozen droplets (state (3)) would stick together and liquid (not supercooled) droplets (state (1)) would probably merge into a single larger droplet before reaching camera level. The effect that a collision between supercooled droplets would have on crystallization is uncertain. Supercooled droplets have been observed to merge on a metallic surface without freezing during the process (reference 3). However, what effect the initial impact in the present case would have on freezing is not known with certainty so the possibility remains that the supercooled droplets may freeze upon impact and thus largely retain their individual shapes. Therefore, state (2) may also exist before collision.

Because of the possibility that collisions play an important part in the growth of rain droplets from cloud droplets through the accretion of smaller droplets (reference 11) and in the crystallization of supercooled clouds, it is desirable to compare the observed frequency of collision obtained from the photographic data (tables I and II) with the computed frequency obtained by the use of theoretical collection efficiencies from reference 11. The average number of collisions by a droplet of diameter S falling 100 centimeters among smaller falling droplets of diameter c was computed. The method of computation is presented in appendix B. Because of the small amount of collision data available, it was necessary to group the photographic data. The grouped computed sums of the average number of droplets in a given size range collected by droplets of size S were compared, therefore, with the similarly grouped data (converted to a 100 cm fall and weighted according to the number of photographs taken at each temperature) obtained from the photographs. The computations for droplets of size S falling among smaller falling droplets in the size ranges from 11.5 to 23.0 microns and 23.0 to 57.6 microns are compared with the experimentally observed values in figure 8. The calculated and observed average number of droplets collected by a larger falling droplet are in good general agreement as to order of magnitude when it is considered that the following uncertainties were present: (1) Only a small amount of collision data was obtained, (2) coalescence and bounce off or both may have been taking place in an unknown fraction of the collisions, (3) the droplet density in the duct was determined at camera level and may not have been representative of conditions in the entire length of the duct, (4) an unknown portion of the aggregates of droplets may have

been so oriented with respect to the camera that they formed circular images and thus were not included in the collision statistics, and (5) a portion of the noncircular images classified as type II may have been due to collisions and thus were not included.

Freezing temperature statistics. - Whereas the photographic method used in this investigation permitted a gross statistical evaluation of the relation between droplet size and freezing temperature, a detailed study of the dependence of freezing temperature on droplet size by this method was impractical for two reasons: (1) The relatively small volume of field of view of the camera provided only a small number of droplets in sharp focus per 8- by 10-inch negative. (2) Inasmuch as each droplet was not observed throughout its entire cooling period, small changes in appearance could not be detected and therefore only those droplets with a definite nonspherical shape could be considered as frozen. Since these were often only a small fraction of the total number of droplets present, it was likely that a sizeable portion of the droplets with a spherical shape may have been frozen. In spite of these limitations several general conclusions can be drawn from the data presented in tables I and II: (1) At temperatures between 0° and -20° C, no noncircular droplet images were observed, indicating that for droplets smaller than 200 microns in diameter the frequency of occurrence of freezing is very small in this temperature region. (Frequencies too small to be detected in this investigation may, however, be significant in the atmosphere because of the very large number of droplets present in a cloud.) (2) The ratio of the number of noncircular droplet images to the sum of the number of circular plus noncircular droplet images was larger at all temperatures for the large droplet-size group (150 μ) than for the small droplet-size group (82 μ) indicating that the droplet freezing temperature tends to increase with increasing droplet size. (3) The approximate temperature at which irregular droplet images appeared agrees reasonably well with the average temperature of the frequency distribution curves for droplets of corresponding size in reference 3. Thus, the results given in reference 3, for droplets supported on a platinum surface, are at least approximately the same as for free-falling droplets in air.

In addition, photographs taken with no vertical air velocity in the duct at temperatures between -36° and -48.5° C (table II) indicated that a very large number of particles (droplets or crystals) below 20 microns in diameter were present in the duct at temperatures between -36° and -48.5° C. The increase in number of particles was particularly marked between -39° and -48° C. This number was far in excess of the number of droplets below 20 microns photographed at room temperature in still air with the same spray nozzles producing droplets. This phenomenon is apparent from the comparison between the observed droplet-size spectrum at room temperature and the particle-size spectrum observed in the temperature range -36° to -48.5° C presented in figure 9. The

large increase in number of particles can be ascribed to one of the following causes: (1) the growth of small frozen droplets originally too small to be detected, (2) the growth of crystals formed from dendritic splinters, (3) the freezing and subsequent growth of droplets formed on condensation nuclei, and (4) the growth of crystals formed on sublimation nuclei. The temperature range in which these particles appear in large numbers brackets the temperatures (-39° to -41° C) given in references 5 to 7 for the transformation in the laboratory of supercooled clouds of small droplets to ice-crystal clouds. The absence of this effect in the data taken with an updraft of 7 centimeters per second is readily explained by the fact that all particles smaller than 46 microns in diameter were excluded from the duct by upward entrainment in the rising air stream.

CONCLUDING REMARKS

The appearance of protuberances and dendritic frost structures on frozen droplets leads to a hypothesis concerning the transformation of supercooled clouds to ice crystals and a mechanism for the production of precipitation. The pointed protuberances which formed at the top of droplets supported by a metallic surface and froze in a water saturated environment were observed in a previous experiment to be the locations of dendritic crystal growth. The tree-like ice structures observed to grow from such points apparently are so fragile that air currents may break them off in fragments, which can become nuclei for additional individual crystalline particles. The pointed protuberances and other irregularities observed on free-falling droplets may also be the location of fragile dendritic frost structures, which in turn may be a source of small ice-crystal nuclei in the form of splinters or fragments that break off. Some evidence of dendritic growth on frozen droplets is apparent in the photographs of free-falling droplets.

As an example, consider the case of warm droplets at the base of a cumulus cloud which are being carried upward by convection currents. As the air rises and cools, the droplets are eventually supercooled. If the droplets are carried high enough, the droplet temperatures are lowered sufficiently for some of the larger droplets to become frozen. These droplets may then be the source of numerous small ice-crystal splinters. These ice splinters can then grow rapidly by reverse sublimation and in turn break up into additional ice splinters, which cause further crystallization of the cloud and eventual precipitation.

The results obtained with the apparatus described in this report can only be considered as preliminary because of the serious difficulty of separating the effects caused by collisions from those inherent in

the freezing process itself. However, the results obtained do yield significant, if not conclusive, information concerning the shape of droplets frozen in air, which in turn throws some light on the nature of transitions from the liquid to the ice phase in clouds. In addition, the results obtained inspire more confidence in the extrapolation of freezing statistics obtained for droplets supported on a platinum surface to droplets suspended or falling freely in air in a natural cloud.

Lewis Flight Propulsion Laboratory
National Advisory Committee for Aeronautics
Cleveland, Ohio

APPENDIX A

DETERMINATION OF DROPLET TEMPERATURE

A droplet falling through the cold vertical duct is cooled by convective heat transfer, radiation, and evaporation. The temperature of the droplet upon reaching the bottom of the duct depends on the rate of heat transfer from the droplet to the surroundings and on the time for the droplet to fall the length of the duct. Because the droplets originate from a spray and therefore have some unknown initial velocity as they enter the duct, the final temperatures of droplets falling through the duct at terminal velocity are computed to show that the final temperature is negligibly different from environmental temperature. If the droplets actually spend more than the computed time in the duct (based on the terminal velocity of the drop), the computed values would indicate a greater temperature difference than the actual existing difference. In computing the temperature difference between the droplet and its environment at camera level, the duct-air temperature will be assumed to be uniform and equal to the average temperature of the two lower thermocouples, which usually differed by less than 1° C. Inasmuch as both radiative heat losses (which are small at temperatures below 0° C) and evaporative heat losses tend to accelerate the rate of cooling (particularly in the upper portion of the duct) over that which would occur because of convective heat transfer alone, these losses will be neglected for simplicity of calculation because only the order of magnitude of the temperature difference between droplet temperature and air temperature at camera level is desired. If the final droplet temperatures computed using only the convective heat-transfer losses are negligibly different from the environment, the actual temperatures should certainly be negligibly different.

The differential equation of convective heat transfer from a droplet to its environment is obtained by equating the heat transfer through the droplet surface to the change in heat content of the droplet. Because the water droplets are less than 200 microns in diameter, the temperature can be assumed to be the same throughout the droplet volume at any instant of time, therefore

$$4\pi a^2 h\theta \, dt = -\frac{4}{3}\pi a^3 c\rho \, d\theta \qquad (A1)$$

where a is droplet radius, h is coefficient of heat transfer at the droplet surface, θ is the temperature difference between the droplet and surrounding air, t is the time, c is the heat capacity of water, and ρ is the density of water. The values of ρ, c, and h are assumed constant for the temperature range considered. The solution of equation (A1) is

$$\theta = \theta_0 e^{-3ht/c\rho a} \tag{A2}$$

which yields the temperature difference as a function of time. The initial temperature difference is θ_0.

The parameter h is obtained from the Nusselt number for spheres. Considerable experimental work has been done on the determination of Nusselt number as a function of Reynolds number and has been summarized by G. C. Williams at M.I.T. and is partly summarized in reference 12. According to Williams, the Nusselt number increases with Reynolds number for values of Reynolds number above 20. For Reynolds numbers below 20, the Nusselt number approaches 2. An equation for Nusselt number which fits quite well the experimental values summarized by Williams is

$$N = 2 + 0.219\ Re^{0.64} \tag{A3}$$

where $N = \frac{2ah}{k}$ is the Nusselt number and $Re = \frac{2aV\rho_a}{\mu}$ is the Reynolds number. Also, k is the thermal conductivity of air, μ is the dynamic viscosity of air, V is the air velocity (with respect to the sphere), and ρ_a is the air density. In the computation of N and h the following values of k, μ, and ρ_a at -20° C as obtained from reference 13 were substituted in equation (A3):

$$k = 5.45\times10^{-5}(cal)(cm^{-1})(sec^{-1})(^{\circ}C^{-1})$$

$$\mu = 1.615\times10^{-4}(g)(cm^{-1})(sec^{-1})$$

$$\rho_a = 1.3769\times10^{-3}(g)(cm^{-3})$$

The velocity V is assumed to be the terminal velocity of a droplet. The terminal velocity as a function of droplet size at an air temperature of -20° C and an air pressure of 75 centimeters of mercury has been computed from the modified Stokes' law equation

$$V = \frac{2}{9}\frac{a^2\rho g}{\mu K} \tag{A4}$$

where $K = \frac{C_D Re}{24}$ represents the effect of variation in drag force on the droplet with variation in velocity and C_D is the drag coefficient for a sphere. When $2a$ is less than 50 microns, K is practically 1 and equation (A4) becomes essentially Stokes' law. The value of K is tabulated as a function of Reynolds number in reference 11. The terminal velocity as a function of droplet diameter has been computed by successive approximation from this table and equation (A4).

The Reynolds number, Nusselt number, and h have been successively computed from the terminal velocity. Also, the time for droplets of a given size to travel the length (127 cm) of the vertical duct at terminal velocity has been computed. Then the ratio θ/θ_0 has been computed for two duct-air velocity conditions and is given in figure 4.

APPENDIX B

DROPLET COLLISION CALCULATIONS

Among the photographs taken at air temperatures below -20° C there are a small number of images that appear to be the result of collisions between partly frozen droplets. These, however, constitute a considerable percentage of the noncircular droplet images. A statistical tabulation of the number of droplet images classified into several categories including collisions is given in tables I and II. Computations have been made of the probabilities of collision in order to determine the plausibility of the statistical results.

The average number of droplets $N_{S,c}$ of a given size c colliding with a droplet of diameter S is given by

$$N_{S,c} = E_{S,c} (L_S - L_c) A_S n_c \tag{B1}$$

where

$E_{S,c}$ collection efficiency for droplet of diameter S falling in air containing smaller droplets of diameter c

L_S length of fall of droplet of diameter S

L_c length of fall of droplet of diameter c in time required for droplets of size S to fall a distance L_S

A_S cross-sectional area of droplet of diameter S

n_c number of droplets per cubic centimeter of diameter c present in path of falling droplet of diameter S

The collection efficiency $E_{S,c}$ is obtained from reference 11.

The length of fall for droplets of diameter S was arbitrarily chosen as 100 centimeters and the corresponding length of fall L_c for droplets of diameter c was computed from

$$L_c = 100 \frac{V_c}{V_S} \tag{B2}$$

where

V_c terminal velocity of droplet of diameter c

V_S terminal velocity of droplet of diameter S

Terminal velocities can be used in the calculations because the time required to reach terminal velocity for droplets smaller than 200 microns is a small fraction of a second.

The number of droplets per cubic centimeter n_c of size c was obtained from the photographs by dividing the number of droplet images in a given size range of mean diameter c by the total volume of field photographed.

Because of the small amount of collision data available it was necessary to group the data. Therefore, the grouped computed sums of the average number of droplets in a given size range collected by droplets of size S were compared with the similarly grouped data (converted to a 100 cm fall and weighted according to the number of negatives at each temperature) from the photographs. A comparison between computed and observed frequency of collision is presented in figure 8.

REFERENCES

1. Dorsey, N. Ernest: The Freezing of Supercooled Water. Trans. Am. Phil. Soc., vol. 38, pt. 3, new ser., Nov. 1948, pp. 247-326.

2. Heverly, J. Ross: Supercooling and Crystallization. Trans. Am. Geophys. Union, vol. 30, no. 2, April 1949, pp. 205-210.

3. Dorsch, Robert G., and Hacker, Paul T.: Photomicrographic Investigation of Spontaneous Freezing Temperatures of Supercooled Water Droplets. NACA TN 2142, 1950.

4. Brewer, A. W., and Palmer, H. P.: Freezing of Supercooled Water. Proc. Phys. Soc. (London), sec. B, vol. 64, pt. 9, Sept. 1, 1951, pp. 765-772.

5. Cwilong, B. M.: Sublimation in a Wilson Chamber. Proc. Royal Soc. (London), ser. A, vol. 190, no. A1020, June 17, 1947, pp. 137-143.

6. Schaefer, Vincent J.: The Production of Clouds Containing Supercooled Water Droplets or Ice Crystals Under Laboratory Conditions. Bull. Am. Meteorological Soc., vol. 29, no. 4, April 1948, pp. 175-182.

7. Fournier D'Albe, E. M.: Some Experiments on the Condensation of Water Vapor at Temperatures Below 0° C. Quarterly Jour. Roy. Meteorological Soc., vol. 75, no. 323, Jan. 1949, pp. 1-14.

8. Young, Allen E., McCullough, Stuart, and Smith, Richard L.: Power Unit for High-Intensity Light Source. NACA RM E50K27, 1951.

9. McCullough, Stuart, and Perkins, Porter J.: Flight Camera for Photographing Cloud Droplets in Natural Suspension in the Atmosphere. NACA RM E50K01a, 1951.

10. Blanchard, Duncan C.: A Verification of the Bally-Dorsey Theory of Spicule Formation on Sleet Pellets. Jour. Meteor., vol. 8, no. 4, Aug. 1951, pp. 268-269.

11. Langmuir, Irving: The Production of Rain by a Chain Reaction in Cumulus Clouds at Temperatures above Freezing. Jour. Meteor., vol. 5, no. 5, Oct. 1948, pp. 175-192.

12. McAdams, William H.: Heat Transmission. McGraw-Hill Book Co., Inc., 2d ed., 1942, p. 236.

13. Montgomery, R. B.: Viscosity and Thermal Conductivity of Air and Diffusivity of Water Vapor in Air. Jour. Meteor., vol. 4, no. 6, Dec. 1947, pp. 193-196.

TABLE I - SUMMARY OF DATA TAKEN WITH UPDRAFT VELOCITY OF 7 CENTIMETERS PER SECOND IN DUCT

Average group temperature (°C)	Average image diameter of size range (μ)	Number of droplet images				Number of droplets in each size range attached to colliding drops			Ratio of noncircular to sum of circular plus noncircular images[a]	Average image diameter of entire group (μ)	Average ratio of noncircular to sum of circular plus noncircular images in entire group[a]
		Total	Circular	Noncircular (type II)	Collisions (type I)	<57	57-115 (μ)	>115			
Higher than -20	51.9	0	0	0	0	0	-	-	0	82	0
	63.4	4	4	0	0	0	0	-	0		
	74.9	17	17	0	0	0	0	-	0		
	86.4	13	13	0	0	0	0	-	0		
	98.1	9	9	0	0	0	0	-	0		
	109.6	10	10	0	0	0	0	-	0		
	126.8	9	9	0	0	0	0	0	0	150	0
	138.3	17	17	0	0	0	0	0	0		
	161.3	3	3	0	0	0	0	0	0		
	184.3	3	3	0	0	0	0	0	0		
-27(±4°)	51.9	8	8	0	0	0	0	-	0	82	0.127
	63.4	17	14	1	2	2	0	-	.067		
	74.9	19	16	2	1	1	0	-	.111		
	86.4	18	15	0	3	2	1	-	0		
	98.1	17	12	4	1	1	0	-	.250		
	109.6	16	10	5	1	0	1	-	.333		
	126.8	17	14	1	2	1	1	0	0.067	150	0.222
	138.3	17	10	4	3	3	1	0	.286		
	161.3	10	5	2	3	0	3	0	.285		
	184.3	5	3	1	1	0	1	0	.250		
-33(±2°)	51.9	5	5	0	0	0	-	-	0	82	0.180
	63.4	15	12	2	1	1	0	-	.143		
	74.9	14	11	2	1	1	0	-	.154		
	86.4	21	16	4	1	1	0	-	.200		
	98.1	28	19	8	1	0	1	-	.296		
	109.6	17	10	4	3	0	2	-	.286		
	126.8	16	11	2	3	1	1	0	0.153	150	0.323
	138.3	24	18	6	0	0	0	0	.250		
	161.3	11	7	2	2	0	1	0	.222		
	184.3	3	1	2	0	0	0	0	.666		
-48(±4°)	51.9	20	18	2	0	0	-	-	0.100	82	0.116
	63.4	37	34	3	0	0	0	-	.081		
	74.9	32	23	7	2	1	2	-	.233		
	86.4	32	27	3	2	2	0	-	.100		
	98.1	20	19	0	1	0	1	-	0		
	109.6	12	9	2	1	0	1	-	.182		
	126.8	16	10	5	1	0	1	0	0.333	150	0.338
	138.3	20	15	3	2	0	1	1	.167		
	161.3	21	11	6	4	1	2	0	.353		
	184.3	6	2	2	2	2	0	1	.500		

[a]Images of colliding droplets (type I) were not used in determination of this ratio because of impossibility of determining whether a collecting droplet or a collected droplet was frozen first.

TABLE II - SUMMARY OF DATA TAKEN WITH NO UPDRAFT IN DUCT

Average group temperature (°C)	Average image diameter of size range (μ)	Number of droplet images				Number of droplets in each size range attached to colliding drops (μ)				Ratio of noncircular to sum of circular plus noncircular images[a]	Average image diameter of entire group (μ)	Average ratio of noncircular to sum of circular plus noncircular images in entire group[a]
		Total	Circular	Noncircular (type II)	Collisions (type I)	<23	23-57	57-115	>115			
-36(±1°)	5.8	0	0	0	--	--	--	-	-	-----	23	0.140
	17.3	15	13	2	0	0	--	-	-	0.133		
	28.8	2	2	0	0	0	0	-	-	0		
	40.4	7	5	2	0	0	0	-	-	.286		
	51.9	18	13	2	3	1	2	-	-	0.133	82	0.443
	63.4	22	6	5	11	2	11	-	-	.454		
	74.9	18	6	7	5	1	5	1	-	.538		
	86.4	15	7	4	4	1	3	1	-	.363		
	98.1	6	3	3	0	0	0	0	-	.500		
	109.6	7	1	2	4	2	5	1	-	.667		
	126.8	6	3	3	0	0	0	0	0	0.500	150	0.875
	138.3	5	0	4	1	0	0	0	1	1.000		
	161.3	5	0	4	1	0	1	0	0	1.000		
	184.3	1	0	1	0	0	0	0	0	1.000		
-39(±1°)	5.8	11	6	5	0	--	--	-	-	0.454	23	0.390
	17.3	120	75	42	3	3	--	-	-	.359		
	28.8	57	37	17	3	2	1	-	-	.315		
	40.4	34	17	13	4	2	3	-	-	.433		
	51.9	20	5	11	4	3	3	-	-	0.687	82	0.929
	63.4	17	0	9	8	11	5	0	-	1.000		
	74.9	17	0	8	9	12	5	0	-	.889		
	86.4	14	0	9	5	7	5	1	-	1.000		
	98.1	13	0	9	4	5	2	0	-	1.000		
	109.6	3	0	3	0	0	0	0	-	1.000		
	126.8	2	0	2	0	0	0	0	0	1.000	150	1.000
	138.3	8	0	7	1	1	1	0	0	1.000		
	161.3	5	0	5	0	0	0	0	0	1.000		
	184.3	1	0	1	0	0	0	0	0	1.000		
-48(±1°)	5.8	50	48	2	--	--	--	-	-	0.040	23	0.214
	17.3	514	372	142	0	0	--	-	-	.276		
	28.8	58	30	22	6	6	0	-	-	.423		
	40.4	23	15	2	6	8	0	-	-	.118		
	51.9	14	6	5	3	4	0	-	-	0.455	82	0.868
	63.4	13	1	3	9	13	1	0	-	.750		
	74.9	11	0	6	5	12	3	0	-	1.000		
	86.4	3	0	1	2	7	1	0	-	1.000		
	98.1	13	0	11	2	5	0	2	-	1.000		
	109.6	5	0	5	0	0	0	0	-	1.000		
	126.8	8	0	8	0	0	0	0	0	1.000	150	1.000
	138.3	0	0	0	0	0	0	0	0	-----		
	161.3	3	0	3	0	0	0	0	0	1.000		
	184.3	0	0	0	0	0	0	0	0	-----		

[a]Images of colliding droplets (type I) were not used in determination of this ratio because of impossibility of determining whether a collecting droplet or a collected droplet was frozen first.

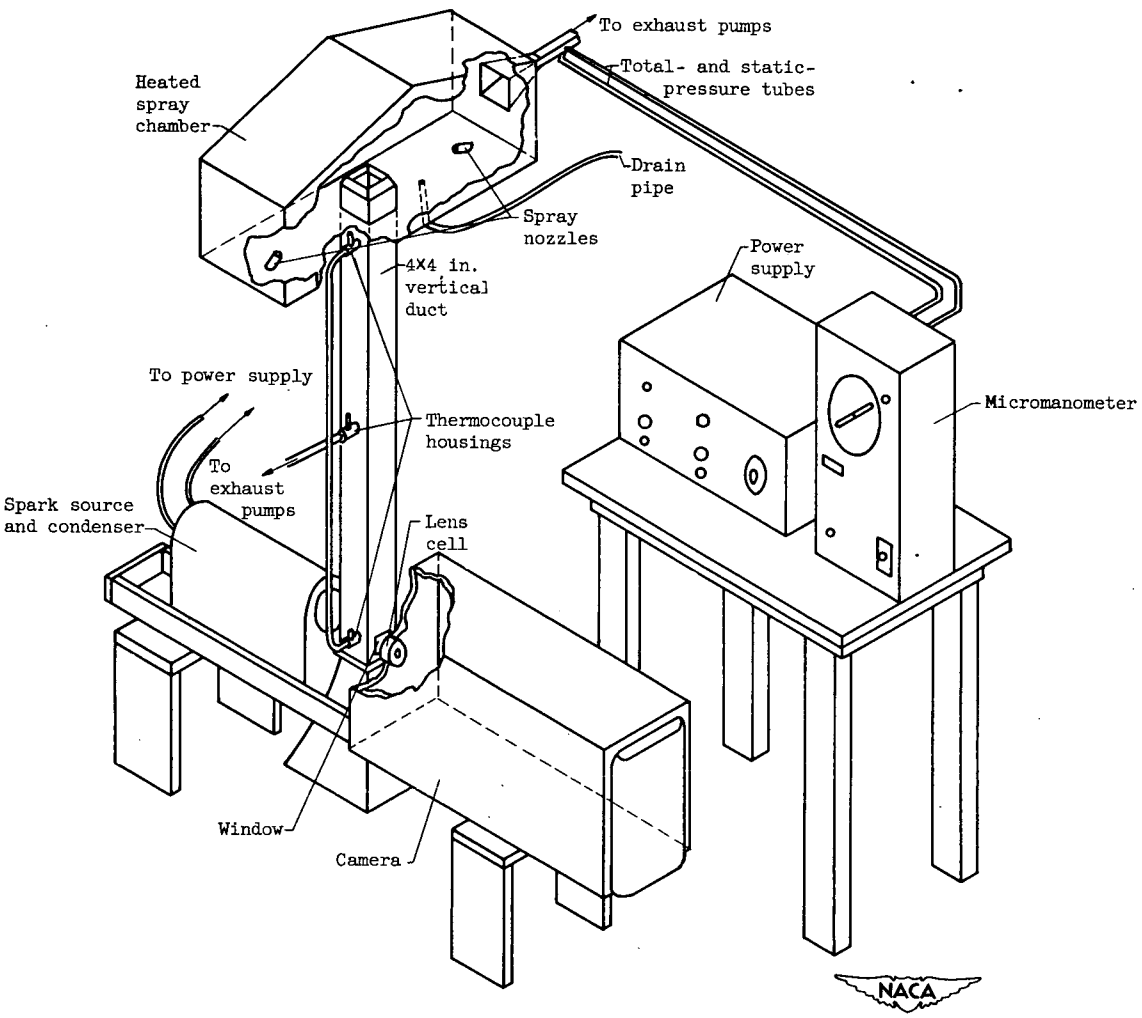

Figure 1. - Schematic drawing of apparatus.

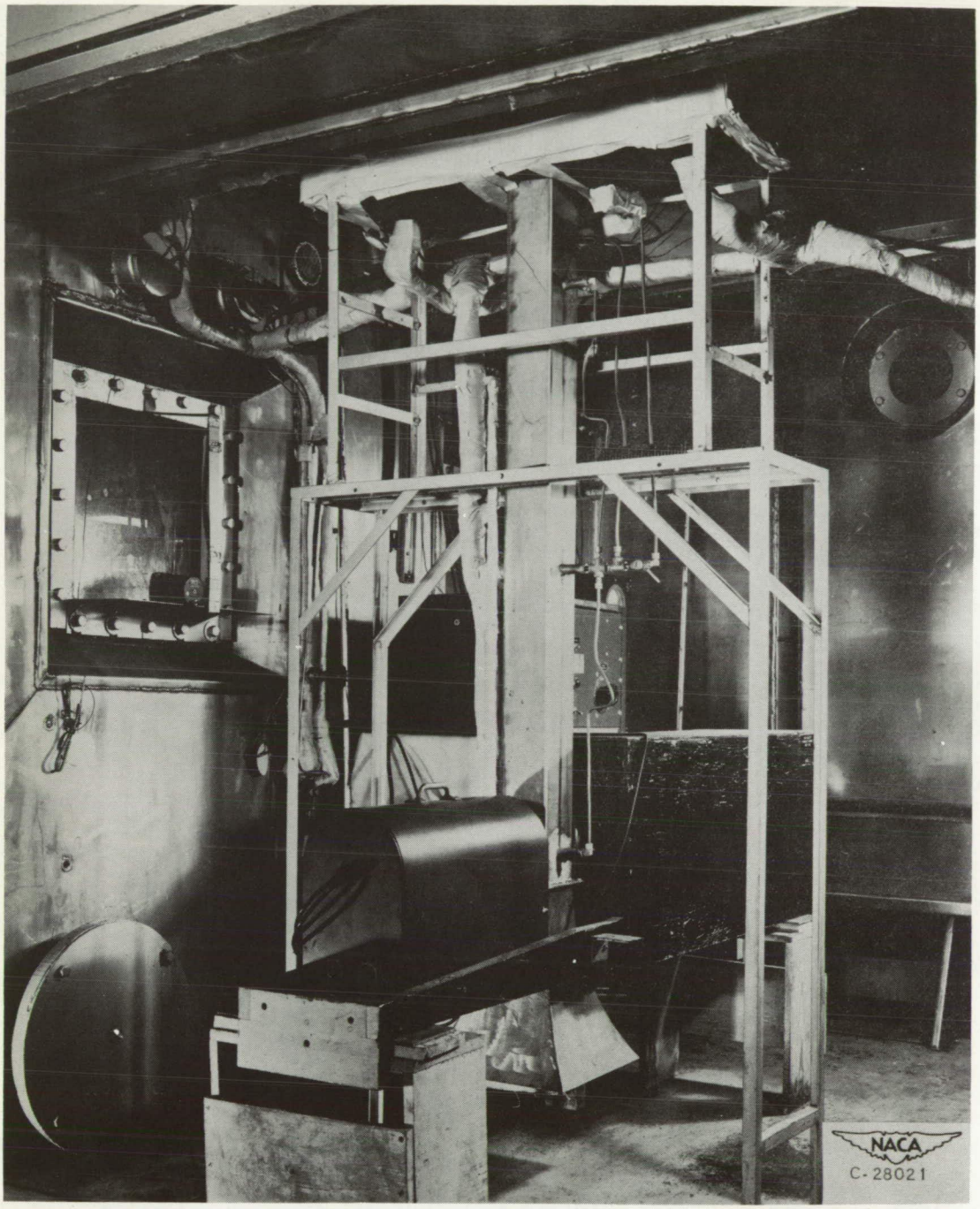

Figure 2. - Apparatus in place in large refrigeration chamber.

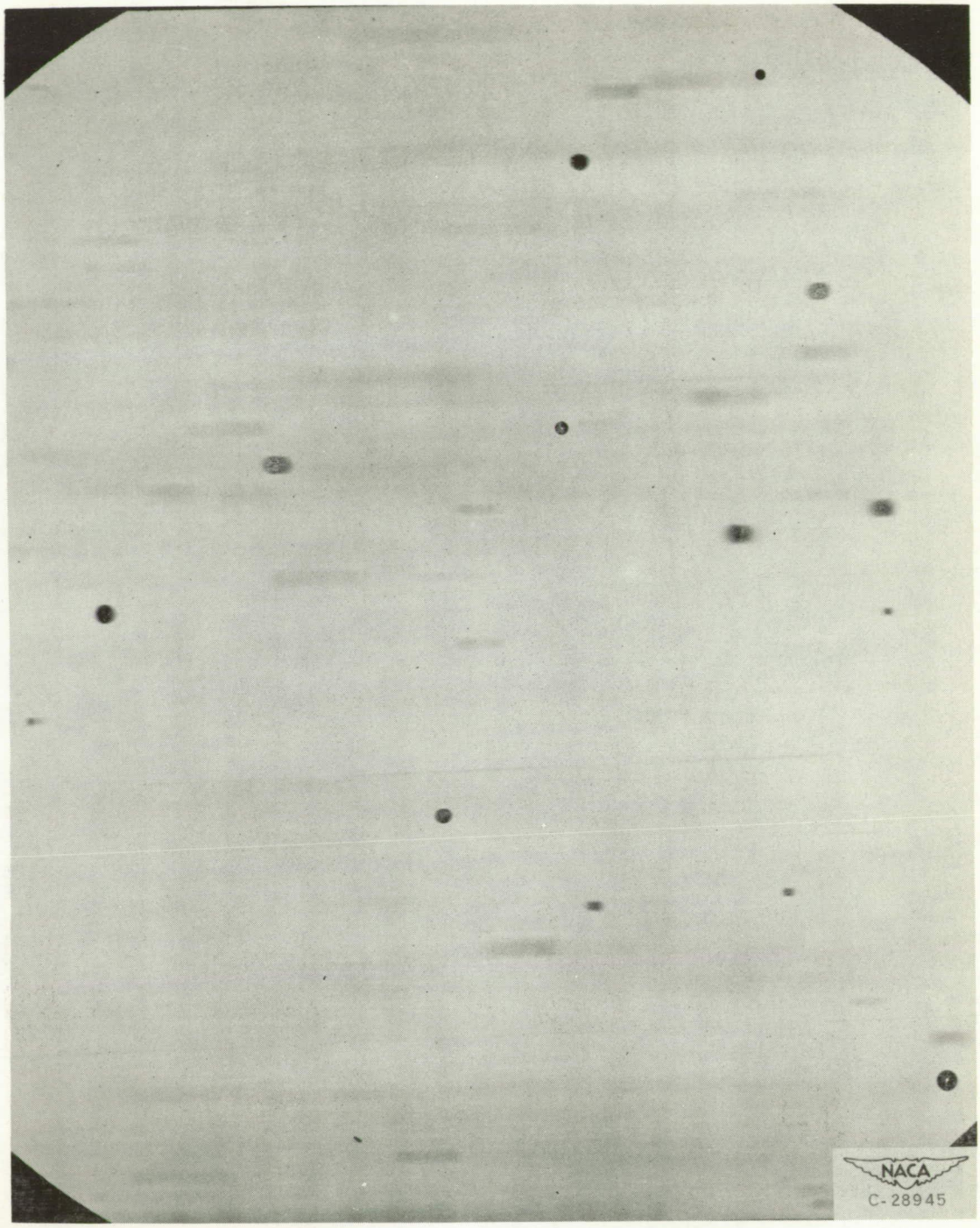

Figure 3. - Droplet images at room temperature. Approximately 18X.

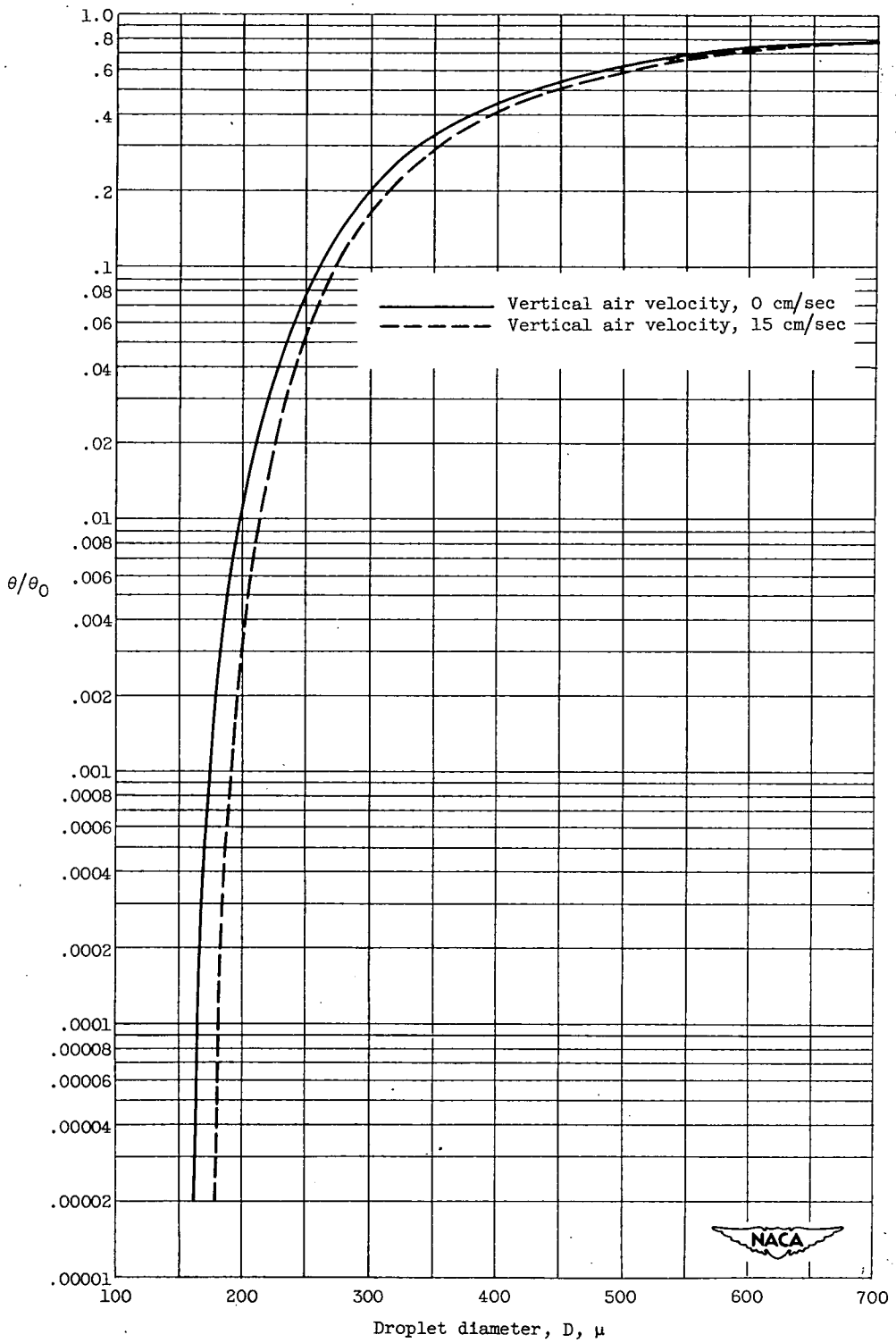

Figure 4. - Ratio of final temperature difference between droplet temperature and duct-air temperature to initial temperature difference θ/θ_0 for droplets falling 127 centimeters at terminal velocity for various droplet diameters.

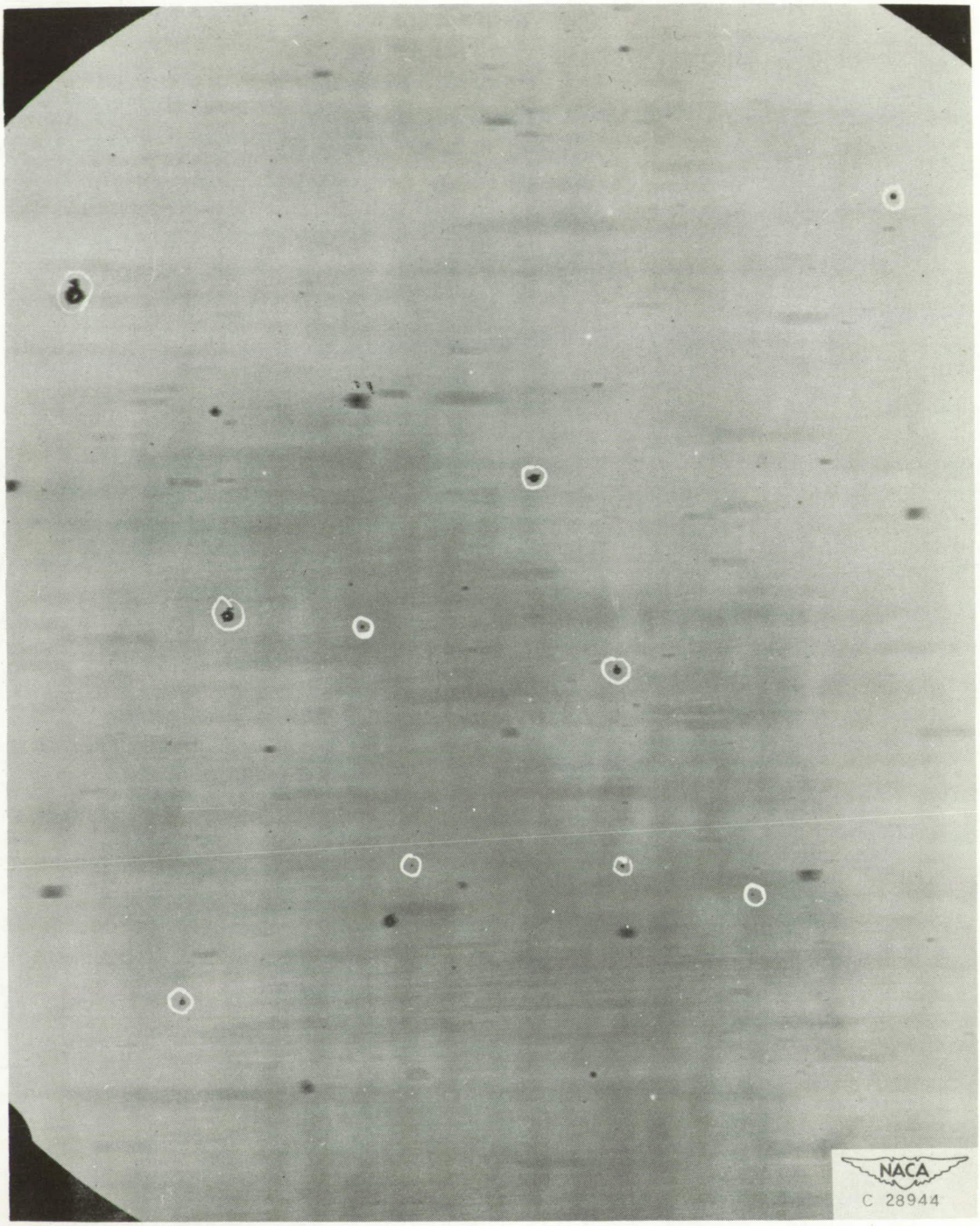

Figure 5. - Droplet images obtained at temperature of -39° C. Approximately 18X.

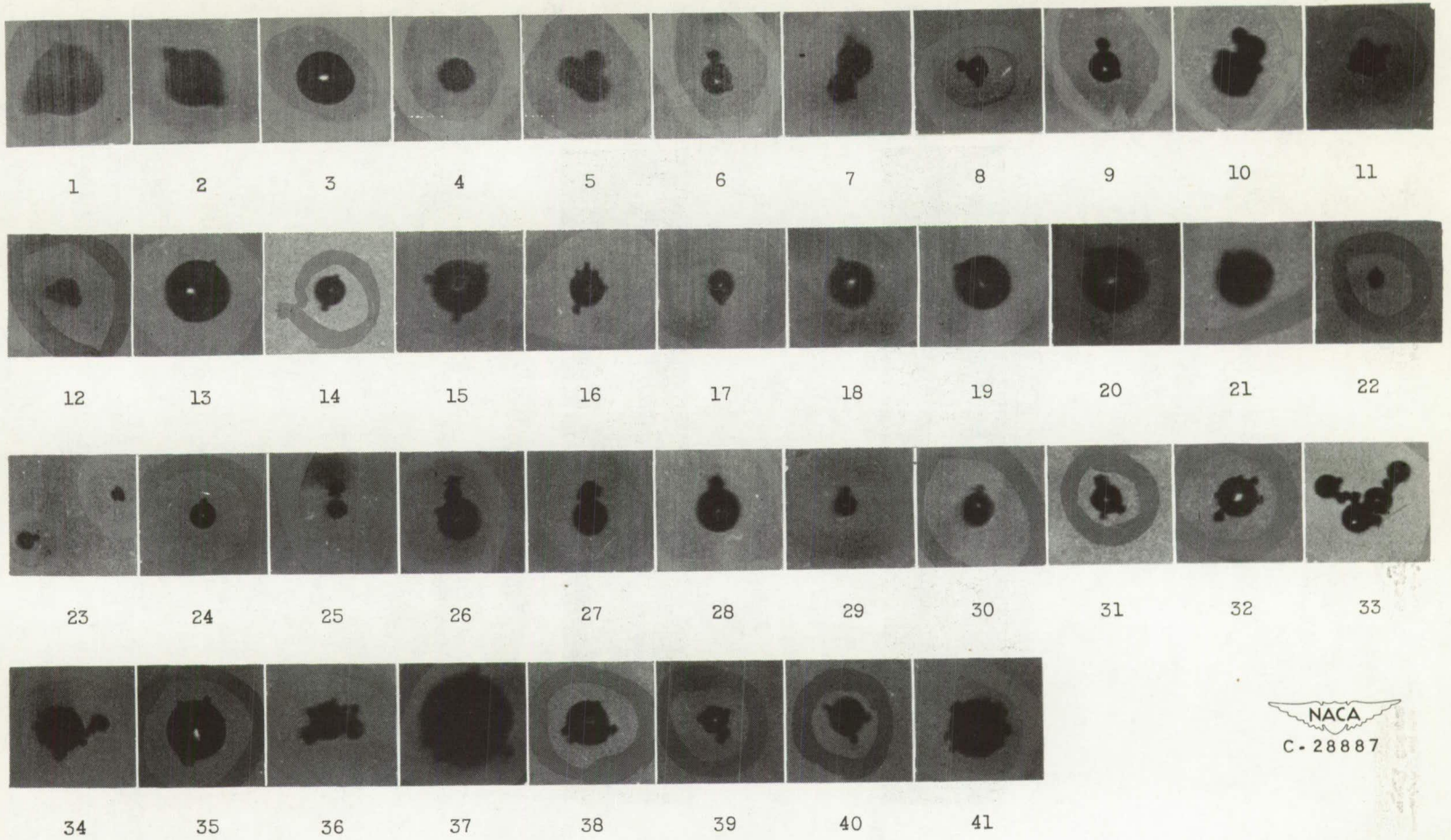

Figure 6. - Droplets frozen while falling freely in still air at temperatures between -36° C and -48° C. Approximately 70X.

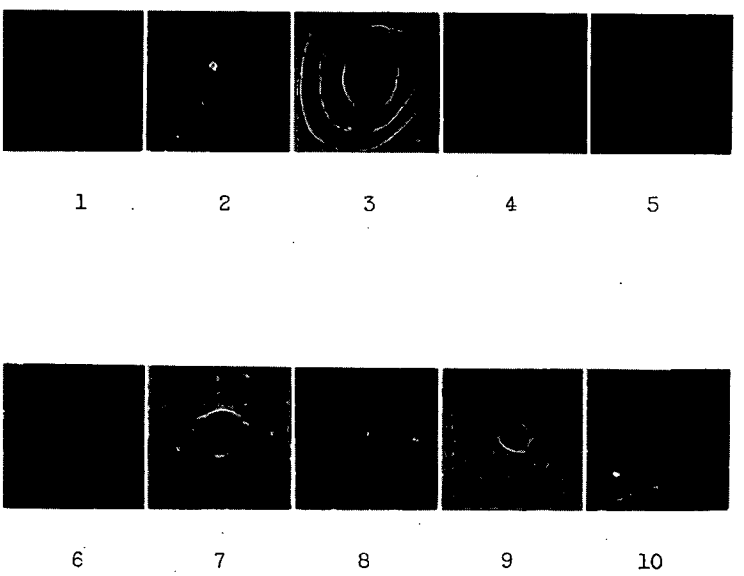

Figure 7. - Droplets frozen while falling freely in column of air with updraft of 7 centimeters per second and air temperature range of -25° to -51° C. Approximately 70X.

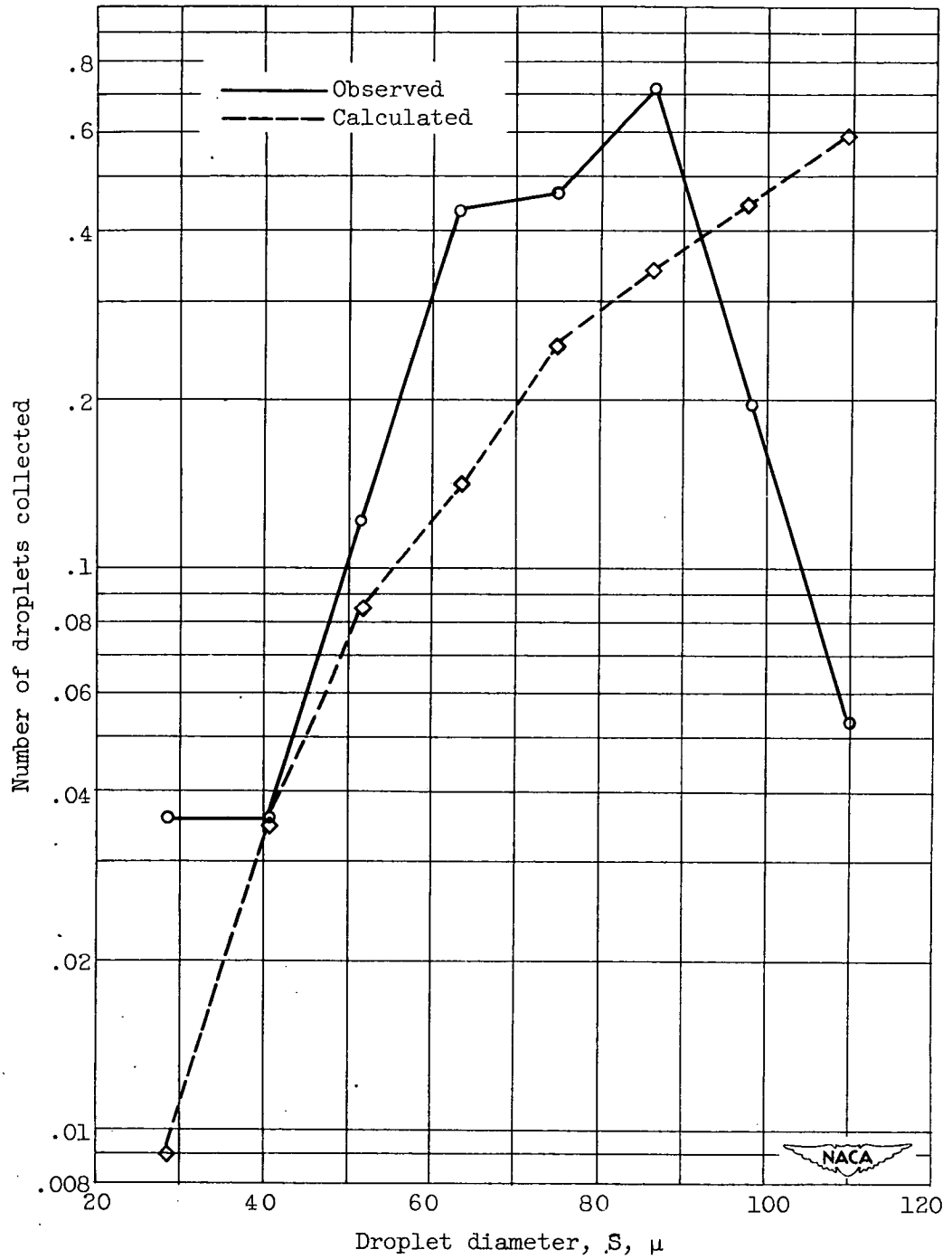

(a) Collected droplets in diameter range from 11.5 to 23.0 microns.

Figure 8. - Comparison of observed and calculated average number of droplets collected by droplet of diameter S falling 100 centimeters in still air among smaller falling droplets.

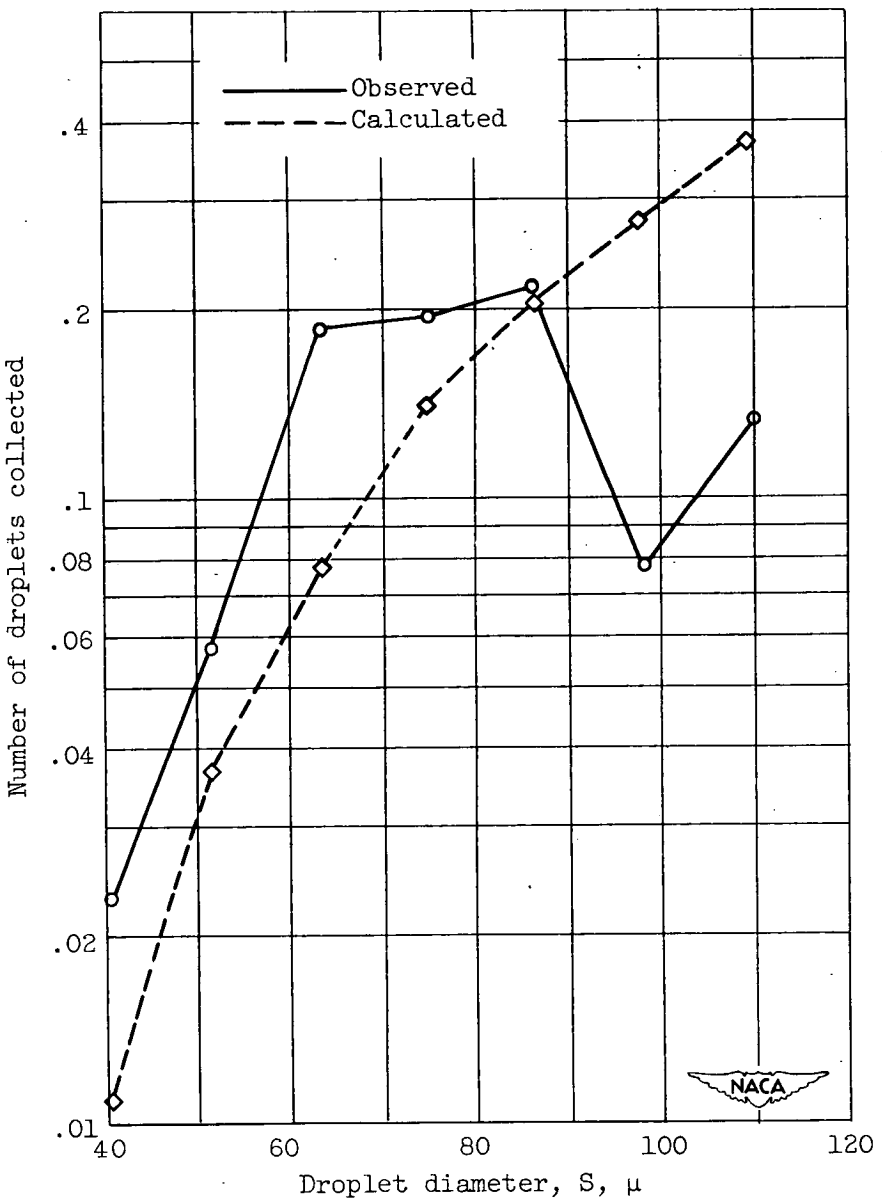

(b) Collected droplets in diameter range from 23.0 to 57 microns.

Figure 8. - Concluded. Comparison of observed and calculated average number of droplets collected by droplet of diameter S falling 100 centimeters in still air among smaller falling droplets.

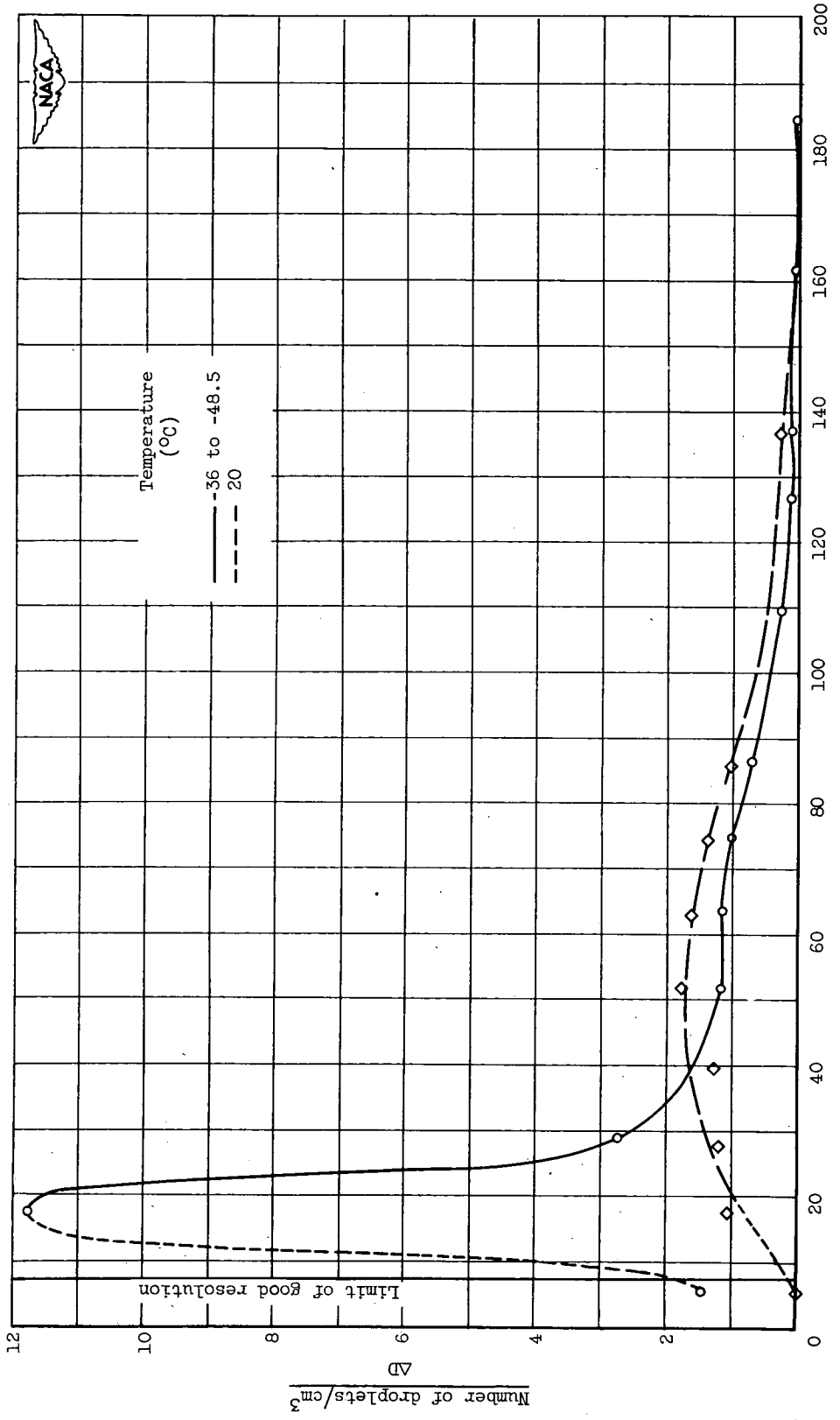

Figure 9. - Distribution of droplet sizes in duct at room temperature and distribution of average droplet sizes in temperature range from -36° to -48.5° C. No vertical air velocity in duct.